

Reliability-based design optimisation of structural systems using high-order analytical moments

Arvind Rajan^{1,*}, Fu Jia Luo², Ye Chow Kuang^{1,3}, Yu Bai², Melanie Po-Leen Ooi³

¹School of Engineering, Monash University Malaysia, Bandar Sunway 47500, Malaysia

²Department of Civil Engineering, Monash University, Clayton, Victoria 3800, Australia

³School of Engineering, University of Waikato, Hamilton, New Zealand

Abstract

Reliability-based design optimisation paradigm has become increasingly popular to achieve economical yet safer structural designs. However, within the iterative optimisation procedure, it is a challenging problem to simultaneously satisfy both, accuracy and computational efficiency of reliability analysis, particularly for nonlinear or large design problems. Addressing the shortcomings of the mainstream reliability estimation methods, this paper presents a new reliability-based design optimisation method that combines an analytical high-order moment-based uncertainty evaluation with an efficient response surface modelling. The proposed framework allows for the precise calculation of reliability through accurate high-order moments. The fast and accurate reliability estimation in combination with efficient sampling, in turn, reduces the total number of finite element analysis in achieving the final design. The proposed moment-based design optimisation methodology was tested on problems ranging from the design of a simple cantilever to a three-dimensional multistorey steel structure. It outperforms the mainstream methods with higher accuracy and lower computational burden especially when applied to a highly nonlinear numerical problem.

Keywords: Method of moments; Reliability; Optimisation; Structural design; Genetic programming; Maximum entropy.

*Corresponding author

Email address: arvindrajan92@gmail.com (Arvind Rajan)

1. Introduction

The method to perform reliability analysis within the large-scale design and optimisation of structural systems is important for the creation of safer and more reliable structures. Design engineers must adhere to engineering building codes which provide information on the reliability of individual elements (such as beams and columns) during the design phase. Finding the overall reliability of the structure while accounting for component and operational uncertainties is a rather complex undertaking. To date, the standard procedure to find the global structural reliability has not been outlined in building codes as it is not a straightforward task [1, 2]. This is because a realistic structure consists of many different elements and the prediction of their dynamic interactions requires the use of computationally intensive simulation through the *finite element method* (FEM) [3].

Addressing the need, innovative techniques for global reliability assessment were developed and are often used to identify the optimal structural designs. This paradigm is commonly known as *reliability-based design optimisation* (RBDO) [4]. RBDO is a probabilistic optimisation that accounts for the overall system uncertainties when selected performance (or limit-state) functions of a structure, normally the *serviceability limit-state* (SLS) and *ultimate limit-state* (ULS), are evaluated. As a result, the RBDO methodology enables a high-quality design that addresses cost-performance trade-off explicitly while at the same time considering the overall system reliabilities.

In a traditional deterministic design optimisation problem where the inherent uncertainties are not considered, the design problem formulation can be expressed mathematically as:

$$\begin{aligned} \text{minimise} & : f(\mathbf{d}), \\ \text{subject to} & : g_i(\mathbf{d}) \leq 0 \text{ for } i = 1, \dots, m, \\ \text{where} & : \mathbf{d}^L \leq \mathbf{d} \leq \mathbf{d}^U, \end{aligned} \tag{1}$$

whereby $f(\cdot)$ is the objective function (which is often the weight or cost of a structure) to be minimised, \mathbf{d} is the vector of design variables with lower bound \mathbf{d}^L and upper bound \mathbf{d}^U , $g_i(\cdot)$ is the

22 i th performance function (which represents the physical performance criterion to be satisfied), and m
 23 is the number of performance functions. In some literature, e.g., [5-8], this deterministic problem is
 24 also referred to as *performance-based design optimisation* where the performance constraints
 25 correspond to SLS and ULS constraints adhering to specific building guidelines.

26 The RBDO, on the other hand, includes probabilistic reasoning into (1), given as:

$$\begin{aligned}
 &\text{minimise} && : f(\mathbf{d}), \\
 &\text{subject to} && : \Pr[g_i(\mathbf{d}, \mathbf{X}) \leq 0] > \Phi(\beta_i) \text{ for } i = 1, \dots, m, \\
 &\text{where} && : \mathbf{d}^L \leq \mathbf{d} \leq \mathbf{d}^U,
 \end{aligned} \tag{2}$$

27 whereby \mathbf{X} is the vector of random variables, $\Phi(\cdot)$ is the normal cumulative distribution function, and
 28 β_i is the i th target reliability index corresponding to performance function $g_i(\cdot)$. Here, the design
 29 vector \mathbf{d} may consist of deterministic parameters and/or parameters related to the random variables \mathbf{X} ,
 30 e.g., $\mathbf{d} = E[\mathbf{X}]$ where $E[\mathbf{X}]$ is the expectation of \mathbf{X} . The probability expression $\Pr[g_i(\mathbf{d}, \mathbf{X}) \leq 0]$ in (2)
 31 can be explicitly expressed as (3):

$$\Pr[g_i(\mathbf{d}, \mathbf{X}) \leq 0] = \int \dots \int_{g_i(\mathbf{d}, \mathbf{X}) \leq 0} f_{\mathbf{X}}(\mathbf{x}) \, d\mathbf{x}, \tag{3}$$

32 whereby \mathbf{x} denotes the realisations of random variables \mathbf{X} , and $f_{\mathbf{X}}(\cdot)$ is the joint probability density
 33 function of \mathbf{X} . Generally, the exact computation of the reliability constraint in (3) cannot be done in
 34 reasonable amount of time for multivariate nonlinear systems, therefore numerical approximations are
 35 commonly employed.

36 Numerous variations of *most probable point* (MPP)-based methods [4, 9, 10] have become some
 37 of the most efficient and simplest methods to compute the reliability constraints in RBDO. In some
 38 literature [11-15], *metamodels* (or surrogate models) are employed to approximate the input-output
 39 relationship followed by sampling methods to approximate the reliability such as the *Monte Carlo*
 40 (MC) method [11] and *importance sampling* (IS) [12]. Since early 2000s, an alternative class of

41 methods, known as the *moment-based method* [16-20], emerged as a possible alternative to perform
42 RBDO [21]. A brief but critical literature review on the developments and shortcomings of these two
43 classes of methods is provided in Section 2. Although they offer a tool to compute the integral in (3),
44 these methods have been shown to suffer from low accuracy, poor convergence, or high computational
45 burden.

46 This paper addresses the limitations of the existing methods summarised in Section 2 by
47 synthesising an original moment-based RBDO computational framework using the authors' previous
48 works on analytical moment computation [22, 23] together with robust moment-based distribution
49 fitting [24] techniques for effective reliability analysis in RBDO. The proposed method is presented in
50 detail in Section 3. Section 4 demonstrates that the proposed moment-based method is both faster and
51 more accurate than the existing methods when employed on benchmark problems of vastly different
52 complexities such as a real-world complex structural design problem. Section 5 then concludes with
53 some future work arising from the current study.

54 **2. Reliability-based design optimisation methods**

55 2.1. Most probable point-based methods

56 The use of MPP-based reliability analysis methods in numerous engineering applications
57 through techniques such as the *first-order reliability method* (FORM) and *second-order reliability*
58 *method* (SORM) has become mainstream since the 1990s. The employment of MPP-based methods in
59 the RBDO of structural designs was introduced in the late 1980s [25], which was then promoted
60 through more studies since the early 1990s [26]. Traditionally, these methods utilise two-level
61 optimisation loops whereby the outer loop is used for the design variable and the inner loop is used to
62 find the reliability index. In order to overcome the high computational cost involved in such double-
63 loop approaches, innovative numerical methods with improved computational efficiencies were later
64 introduced. For instance, the inner loop's reliability analysis was replaced with Karush-Kuhn-Tucker
65 conditions [27]; a decoupled approach was introduced to replace the double loop framework [28]; and

66 a sequential approximate programming strategy, known as the *performance measure approach* (PMA)
67 [29], was proposed to replace the original problem of finding the reliability index with a new
68 formulation. Later, the PMA was improved with a hybrid analysis [30] for better convergence of
69 reliability analysis. Many more incremental improvements have been introduced for MPP-based
70 reliability analysis over the last decade [4, 31-33].

71 The numerical efficiency of these methods stems from the concept of finding the MPP, which
72 may be interpreted as the most likely point of failure. Pivoting on the MPP, these methods reduce the
73 computational complexity by transforming RBDO formulation from a double-loop probabilistic
74 estimation problem into an approximately equivalent single-loop problem. However, the problem
75 reformulation in terms of the MPP is that it is an approximation that can sometimes result in an
76 unsatisfactory estimate. This has been well-examined in the literature, e.g., [21, 34, 35]. For example,
77 low accuracy was found in the reliability estimation of limit state functions with nonlinearity or non-
78 normal variables; convergence becomes poor in the search of the MPP for high system reliability; and
79 possibilities of non-unique MPPs may lead to inaccurate reliability analysis. In addition, [36]
80 demonstrated that the MPP-based methods could under- or overestimate the reliability depending on
81 the local curvature of the performance function in the neighbourhood of the MPPs. Although the study
82 went on to propose MPP-based dimension reduction method addressing the shortcoming, the results
83 show that it could only reduce the severity of the problem but not remove it.

84 In brief, although various improved techniques for accurate and efficient reliability analysis have
85 been developed over the years, most techniques depend on finding the MPP reliably and efficiently.
86 Section 4 will explore and demonstrate the abovementioned fundamental limitations of the MPP-based
87 approaches.

88 2.2. Metamodel with direct sampling methods

89 In a different line of development in the RBDO literature [11-15, 37-41], metamodels were built
90 using selected samples to approximate the input-output relationship in order to reduce the

91 computational cost. This line of investigation does not exclude MPP techniques, but the combination
92 of MPP and metamodel is relatively rare. This is because direct sampling methods are more reliable
93 than the MPP-based techniques and the computational cost for direct sampling is deemed negligible
94 with the availability of metamodels [11, 12].

95 Many modelling methods such as moving least squares with selective interaction sampling [41],
96 iterative response surface with moving least squares [9], adaptive sparse polynomial chaos expansion
97 [38], support vector machine-based *radial basis function* (RBF) [14], *artificial neural network* (ANN)
98 [13] have been experimented. Once a metamodel has been built, direct sampling methods, such as MC
99 [11] or importance sampling [12], can be used to estimate the reliability. The RBF, polynomial chaos
100 expansion, and ANN approaches were reported to have the tendency of overfitting [39], heavy
101 dependence on design of experiments and polynomial degree [37], and computationally expensive
102 [40], respectively. Kriging modelling and its numerous variations are different from the above methods
103 because it builds a flexible non-parametric model. The reliability can then be estimated from Kriging
104 model using the moment approach [15], the MC method [11], and importance sampling [12].

105 The use of the MC method for reliability analysis has been shown to have adverse effect on the
106 convergence or stability of the optimiser due to the sampling noises [24]. Increasing the MC sample
107 size to reduce the sampling noise, on the other hand, demands disproportionate increase in
108 computational overhead. Importance sampling [11, 12] is an example of a more efficient sampling
109 technique compared to the direct MC method. However, it should be noted here that sampling
110 efficiency is not the primary challenge of using the MC method for design optimisation; rather the
111 primary challenge is the sensitivity of the optimisation convergence with respect to the sampling noise.
112 This will be demonstrated numerically in Section 4.1. In addition, the importance sampling technique
113 comes with the added complication of selecting a suitable sampling distribution. This task is sometimes
114 not straightforward, and a wrong choice has detrimental effects on stability and accuracy [42, 43].
115 Furthermore, existing importance sampling techniques used for reliability analysis are pivoted around

116 the MPP [12] to achieve greater efficiency gains. Section 4 will explore the risk of relying on MPP as
117 a pointer to perform reliability analysis. Section 4 will also go on to demonstrate some limitations of
118 the MC method (in addition to the MPP-based ones) for reliability analysis in RBDO.

119 2.3. Moment-based methods

120 Unlike the MPP-based methods, articles on the use of moment-based methods for reliability
121 analysis in structural systems are scarce. Moment methods have been used to find the reliability from
122 metamodels instead of direct sampling. The first introduction of the approach was by [21] in the early
123 2000s. Since then, more computational-efficient approximations of the high-order moments have been
124 developed. For example, fewer samples for response surface approximation using second-order
125 polynomial models were used in [35] and [44] for moment calculation; a dimension reduction strategy
126 was introduced in [19, 45] to find the high-order moments more efficiently and accurately; and more
127 recent developments by [17, 18, 20] advocate the use of moment-based methods by employing the
128 third- and fourth-moment reliability indexes. These improved reliability analyses are strictly based on
129 the first four moments found using approximations, which are unfortunately numerically susceptible
130 to sampling and approximation errors with increasing order [46].

131 The conventional moment-based methods calculate the statistical moments, typically up to the
132 fourth order, and subsequently use a parametric distribution fitting method [47] to infer the reliability
133 of the output-of-interest. The approach has an advantage of not changing the original problem
134 formulation, and hence, it removes any difficulties associated with finding the MPP and/or
135 approximating the original solution with MPP-mediated ones. Nevertheless, the existing moment-
136 based methods are under scrutiny considering the following limitations [48]: (1) limited numerical
137 precision in the estimated moments leading to incorrect reliability estimates; (2) many more moments
138 (more than four) are required to approximate the probability density function accurately [24]; and (3)
139 the parametric probability model, especially those with unimodal assumption, may not reflect the true
140 nature of the probability distribution under investigation.

141 On the other hand, theoretical investigations [49, 50] show that higher order moments will result
142 in a more accurate reliability computation with quantifiable bounds of uncertainty. These bounds on
143 estimation uncertainty can be calculated non-parametrically using the available moments and is valid
144 under very general conditions. These characteristics are highly valuable to the design and regulation
145 of structural safety, and thus, making the moment-based approach a viable candidate for reliability
146 analysis. In short, these studies favour the use of moment-based methods in reliability analysis on the
147 condition that an accurate tool for moment calculation is available.

148 In authors' previous works, the limitations of the moment-based method were comprehensively
149 addressed with the introduction of novel techniques for analytical moment computation of arbitrary
150 order [22, 23] (thus overcoming the first two limitations) and parametric distribution fitting method
151 that does not rely on a unimodal assumption while still supporting arbitrary order moment [24] (thus
152 overcoming the third limitation). In a recent study [51], the analytical moment computation framework
153 was also shown to be capable of handling performance functions with high nonlinearity and
154 dimensionality (or number of variables). However, to the best of authors' knowledge, these methods
155 have not been formally presented for reliability analysis within the larger RBDO framework.
156 Therefore, the proposed RBDO framework, presented in the Section 3, adopts these techniques and
157 presents a novel high-order analytical moments-based RBDO method.

158 **3. Proposed moment-based RBDO**

159 The preceding section argues that moment-based methods side-step the complications of finding
160 the MPP and convergence of sampling methods in the mainstream RBDO methodologies. This section
161 will show how the high-order moments can be found for an arbitrary system response function in
162 RBDO by combining *polynomial genetic programming* [52] for local metamodeling and recent
163 advancements made in analytical moment-based reliability analysis [22-24]. Note that the latter will
164 be known as *moment-based uncertainty evaluation technique* (MUET) in this paper. The proposed
165 RBDO framework overcomes the abovementioned limitations in the MPP-based methods. Compared

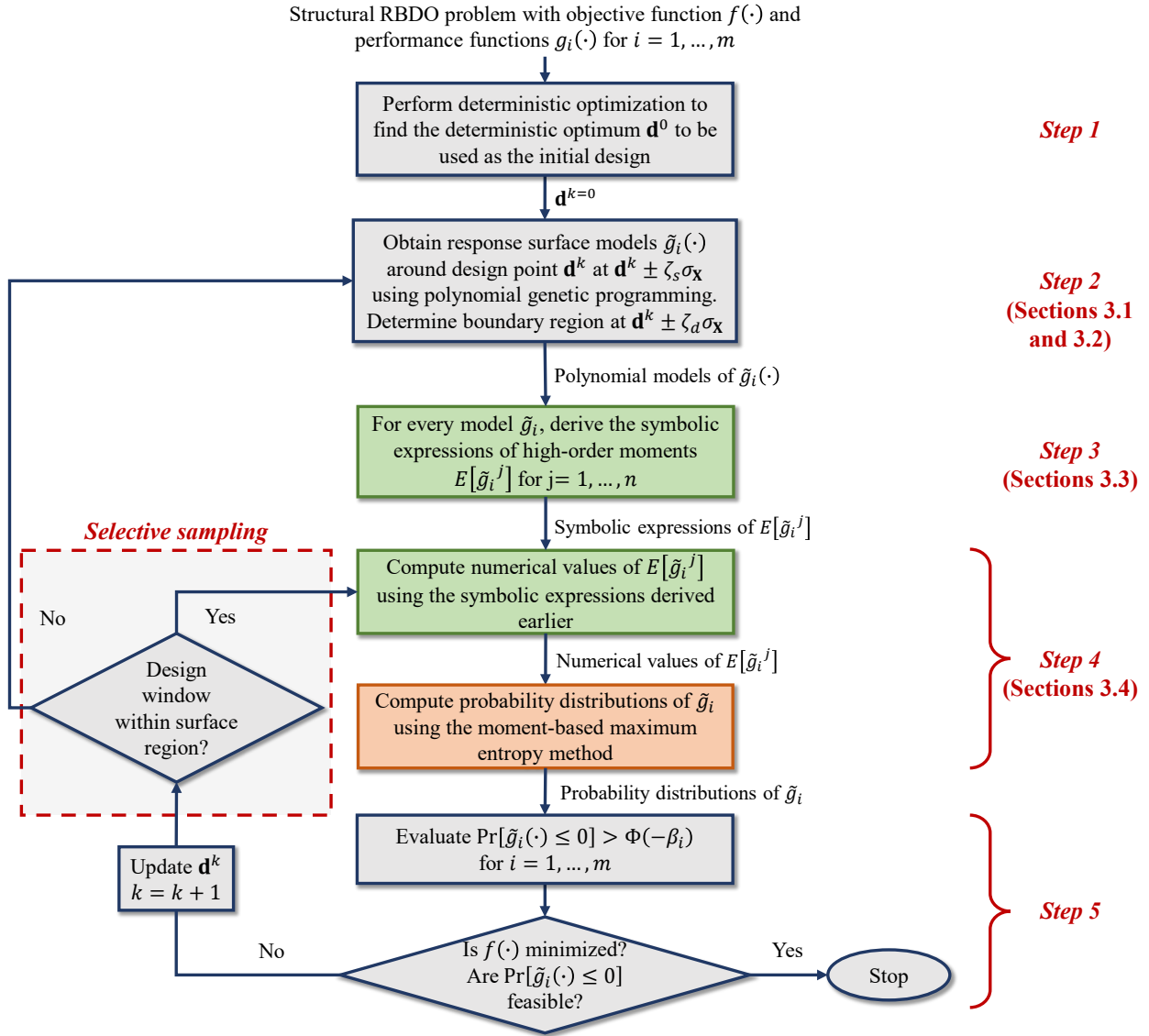
166 to the existing moment-based methods, however, the proposed method allows (1) analytical
167 computation of moments higher than fourth-order for better accuracy and (2) robust distribution fitting
168 that supports more than four moments unlike the mainstream methods [24], thus providing more
169 dependable results.

170 Figure 1 presents the procedural flow of the proposed moment-based RBDO method. Each step
171 will be elaborated in the following subsections. As shown in the flowchart, once the RBDO problem
172 has been formulated by identifying the objective function and performance functions according to (2),
173 the following five steps will be executed:

174 Step 1: Find the deterministic optimum design using the formulation shown in (1) and use it as the
175 initial design $\mathbf{d}^{k=0}$ of the moment-based RBDO, \mathbf{d}^k denotes the design point at k th
176 iteration.

177 Step 2: Model the response surface of the performance function $g_i(\cdot)$ for $i = 1, \dots, m$ using
178 polynomial genetic programming [52] (Sections 3.1) around design point \mathbf{d}^k using surface
179 region constant ζ_s and the vector of standard deviation of the random variables $\sigma_{\mathbf{x}}$, and
180 determine the *design window* for *selective sampling* using the design window constant ζ_d
181 and $\sigma_{\mathbf{x}}$ (Sections 3.2). The *Latin hypercube sampling* [53] is used to build the local
182 response surfaces with sample size $(2N + 1)(m + 1)$, whereby N denotes the total
183 number of (design and random) variables.

184 Step 3: Find the closed form expressions of high-order moments $E[\tilde{g}_i^j]$ for $i = 1, \dots, m$ and $j =$
185 $1, \dots, n$ using the analytical moment propagation framework introduced in [22, 23],
186 whereby $\tilde{g}_i(\cdot)$ denotes the approximated performance function; j denotes the order of the
187 statistical moments used; n denotes the number of high-order moments used. Section 3.3
188 gives a brief overview of the efficient symbolic high-order moments calculation procedure.
189 Evaluate the numerical values of $E[\tilde{g}_i^j]$ for $j = 1, \dots, n$.



190

191 Figure 1. Framework of the proposed moment-based reliability-based design optimisation (RBDO) method. The green and orange
 192 boxes denote the contribution from authors' previous works [22, 23] and [24], respectively, used in the new moment-based reliability
 193 analysis within the proposed RBDO.

194 Step 4: Find the probability distribution of the performance functions using moment-constrained
 195 maximum entropy method [24], presented in Section 3.4.

196 Step 5: Finally, ensure that the constraints, i.e., $\Pr[g_i(\cdot) \leq 0] > \Phi(-\beta_i)$ are met using the
 197 estimated probability distribution while ensuring that the objective function $f(\cdot)$ has been
 198 minimised. If neither of the condition is met, update the design point \mathbf{d}^k for $k = k + 1$
 199 using the chosen optimiser. Then, go to Step 2 if the design window exceeds the response
 200 region; or Step 4 if otherwise (refer Sections 3.2).

201 Note that the choice of optimiser is immaterial to the proposed moment-based RBDO framework.
202 The *sequential quadratic programming* (SQP) approach [54] has been chosen in this study. This is
203 because it is one of the more efficient general-purpose optimisers for nonlinear constrained
204 optimisation that is widely available in most computational platforms. The approach iteratively finds
205 the optimum point that corresponds to minimum/maximum value of the objective function by
206 combining an active set method and Newton’s method while using the derivatives of the objective
207 function as well as the constraints [54]. In this study, SQP is employed with the following settings:
208 central *finite difference method* (FDM) [55] for gradient calculation; and constraint, optimality, and
209 step tolerances of 1×10^{-6} (additional information can be found in MATLAB documentation [56]).

210 In addition, it is also important to state that the MC method can be employed for reliability analysis
211 after the response surface is built. However, as reported in [24], the sampling noise in MC method
212 sometimes creates instability in the optimisation and terminates the optimisation prematurely as the
213 algorithm approaches the final solution. Although it is a rare occurrence, when (and if) it happens, it
214 degrades the quality of the solution in terms of constraints adherence and solution optimality. As a
215 result, the proposed analytical moment method is employed for reliability assessment instead.

216 3.1. Local response surface modelling using polynomial genetic programming

217 It is customary to employ response surface methodologies to build metamodels of the performance
218 functions $g_i(\cdot)$ in (2) [57] for various large-scale optimisation problems. The metamodels enable
219 efficient evaluation of system response when the closed form expression is not available in complex
220 engineering problems. Although there are various techniques available for this purpose, local
221 metamodels using second-order polynomials are some of the most commonly used approaches, even
222 in MPP-based RBDO methods [41, 58]. Furthermore, studies [59, 60] recommend multivariate
223 polynomials to be the preferred metamodel over the RBF, ANN, and Kriging as they are
224 simultaneously accurate, robust, and computationally efficient. The results from these studies have

225 demonstrated that this strategy significantly improves both, the computational efficiency and the
226 accuracy of the RBDO computation simultaneously.

227 Genetic programming is an approach inspired by biological evolution, whereby, using an
228 evolutionary algorithm, a set of model parameters will evolve to optimise the objective function. The
229 use of genetic programming to build metamodels was first reported in the late 1990s [61], whereas the
230 earlier works of using polynomials as the node functions in genetic programming were reported in the
231 early 2000s [62]. A recent study [52] introduced a more accurate and efficient polynomial genetic
232 programming algorithm for response surface modelling, and went on to demonstrate that it can reliably
233 model highly nonlinear functions. A further investigation in [53] then employed the framework to
234 validate its sound application on RBDO of structural systems in combination with MPP-based
235 reliability analysis. This study, however, employed a more recent symbolic genetic programming
236 framework [63] for local response surface modelling due to the availability of a free and open source
237 program.

238 3.2. Selective sampling technique

239 Although response surface modelling using the polynomial genetic programming is superior to the
240 commonly-used second-order polynomials [52], a global model may still lead to inaccurate
241 approximations of the performance functions. The inaccuracy often results in the incorrect evaluation
242 of the probabilistic constraints during the RBDO process [53]. On the other hand, using local surface
243 approximation at every design point would result in a high computational burden. Therefore, in order
244 to maintain both accuracy and computational efficiency simultaneously in the evaluation of the
245 probabilistic constraints, the selective sampling technique introduced in [41] is employed. The
246 selective sampling technique can be perceived as a crossover between the global and local modelling
247 as it determines the need for a new local response surface based on a mechanism using a *surface region*
248 and a *design window* (explained below). As a result, a new local response surface will only be modelled
249 if deemed necessary, which in turn, improves the computational efficiency.

250 For every performance function $g_i(\cdot)$, the response surface is modelled using the Latin hypercube
 251 sampling with a sample size $(2N + 1)(m + 1)$ following [53]. As shown in Figure 1, the proposed
 252 RBDO begins by finding the deterministic optimum $\mathbf{d}^{k=0}$. Then, the localised approximation of the
 253 response surface is performed around the intervals in (4):

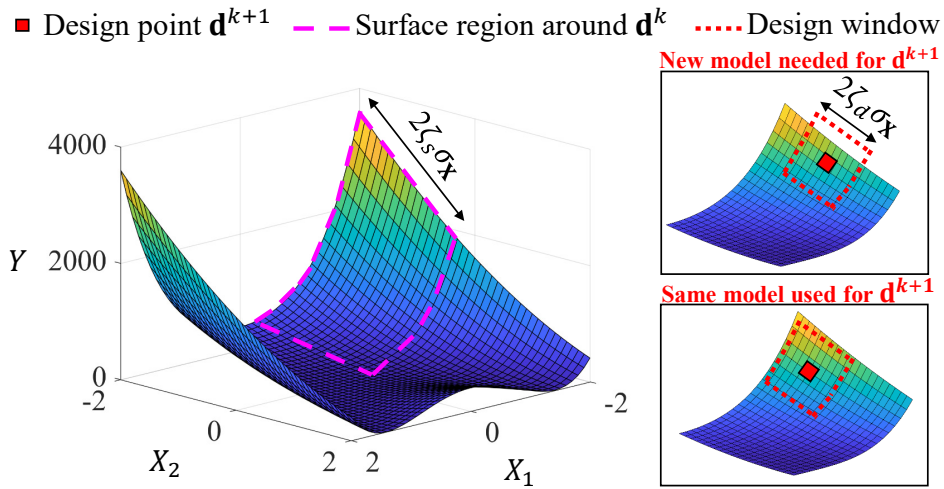
$$\mathbf{d}^k \pm \zeta_s \sigma_{\mathbf{X}}. \quad (4)$$

254 Generally, the value of surface region constant ζ_s is selected based on a multiplicative factor of 1.2-
 255 1.5, which is associated with the target reliability index β used in the optimisation problem. For
 256 example, 1.2β is used for moderately nonlinear problems while 1.5β is used for highly nonlinear ones
 257 [11]. The design window constant, denoted by ζ_d however, is a smaller value ($\zeta_d < \zeta_s$) used for the
 258 selective sampling technique. The mechanism of the technique is illustrated in Figure 2 using the
 259 highly nonlinear Rosenbrock function in (5):

$$g(\mathbf{X}) = 100(X_2 - X_1^2)^2 + (1 - X_1)^2 \quad (5)$$

260 where $-2 < \{X_1, X_2\} < 2$ [64]. This analytical function is chosen because it is often used in
 261 optimisation and reliability analysis literature for the common practice of performance benchmarking
 262 due to its high nonlinearity yet low dimension (which allows for visualisation); however, note that any
 263 continuous and nonlinear analytical function can be adopted to illustrate the mechanism.

264 Assume that a local response surface region (dashed lines) is built around \mathbf{d}^k using the intervals
 265 (4). In the following iteration, the design point \mathbf{d}^{k+1} changes and the need for a new model is
 266 determined using the design window $\mathbf{d}^{k+1} \pm \zeta_d \sigma_{\mathbf{X}}$ (dotted lines). For example, in Figure 2, when the
 267 design window around \mathbf{d}^{k+1} exceeds the existing surface region, a new local response surface is
 268 modelled around \mathbf{d}^{k+1} ; or else, the existing model is used. By doing so, a local response surface need
 269 not be modelled at every iteration, which enhances the overall efficiency of the RBDO process.



270

271 Figure 2. Illustration of the selective sampling technique using the highly nonlinear Rosenbrock function [52]. When the design point's
 272 design window exceeds the surface region, a new model is required, and vice versa.

273 3.3. High-order analytical moments

274 The MUET [22, 23] can be used to precisely calculate the analytic expression of an arbitrary j th
 275 order statistical moments of the approximated performance function \tilde{g}_i , denoted by $E[\tilde{g}_i^j]$. An open
 276 access online calculator was made available for the symbolical computation of the moments, which
 277 alleviates the tedious steps involved in the derivation of the analytical expressions [22]. The framework
 278 supports various probability distributions with finite moments and requires that the performance
 279 function be represented in a general polynomial form (can be found in [52]) to which the metamodels
 280 from the polynomial genetic programming comply. It is also worthwhile to note that other modelling
 281 techniques using multivariate polynomials, such as the polynomial dimensional decomposition [65],
 282 polynomial support vector machine [66], and high-order polynomial approximation [67], also fit into
 283 the general polynomial form; and therefore, they are compatible with the MUET.

284 The analytical framework of the MUET [22, 23] accurately and symbolically calculates the high-
 285 order moments at Step 3 of the proposed framework. As a result, the moments are calculated using a
 286 predetermined finite number of steps by performing simple substitutions of the design point \mathbf{d}^k . This,
 287 in turn, alleviates the computational burden of evaluating the reliability constraints in RBDO since it
 288 does not involve any other iterative process. If the metamodeling technique limits the highest

289 acceptable order of the polynomial, e.g., second-order polynomial [35], this step can be made even
290 faster by building a lookup table. For example, given a certain highest order of polynomial, there will
291 be a finite number of possible polynomial forms. MUET can be executed beforehand to build the table
292 of moment expression for each form, thus saving the MUET computation in the workflow.

293 3.4. Moment-constrained maximum entropy method

294 With the set of statistical moments corresponding to the respective performance functions, an
295 approximate distribution that is consistent with the moments can be found. The moment-constrained
296 maximum entropy method was recently introduced in [24] for uncertainty (or reliability) analysis and
297 has been used to support high-order moment approximation. [24] also showed that the maximum
298 entropy algorithm is generally superior to the other parametric fitting methods, such as the Pearson
299 method. The combined framework of the analytical MUET and the maximum entropy algorithm in the
300 proposed method, therefore, seamlessly complements each other in handling higher order of statistical
301 moments.

302 Compared to the other parametric distribution fitting algorithms, the entropy maximisation
303 principle is consistent with safe handling of uncertainty. It generally favours the distribution with larger
304 spread if there are more than one solution that satisfy the given moment equality constraints. This is
305 an important factor to be considered for safety-critical engineering designs.

306 4. Numerical examples and applications

307 To verify the accuracy and efficiency of the proposed moment-based RBDO framework, it is
308 employed on solving one numerical and three structural RBDO problems of varying complexity.
309 SORM will outperform FORM in some cases but its dependence on curvature information makes it
310 less robust and more difficult to use, hence it is less widely adopted in practice compared to FORM.
311 Therefore the results are compared against different variations of MPP-based FORM methods reported
312 in [55] and [33] as they are normally used as benchmarks in numerous RBDO literature. In this study,

313 the MUET is employed to calculate the moments of the performance functions up to the sixth order
314 ($j = 6$), and the selective sampling method has been employed with $\zeta_s = 4$ and $\zeta_d = 3$.

315 The first problem (in Section 4.1) is a nonlinear numerical problem which minimises the objective
316 function with respect to a constraint function with two design variables. The objective of this
317 experiment is to compare the moment method against the Monte Carlo and Importance Sampling
318 methods as well as the MPP-based strategy commonly used for reliability analysis. The second
319 problem (in Section 4.2) is a simple RBDO problem of a cantilever beam with two design variables
320 and five random variables [55, 68]. The system response is known analytically to enable the discussion
321 of 1) the accuracy and efficiency of the proposed method; and 2) the source of the improved
322 computational efficiency in the proposed method by examining its iteration history. The third problem
323 (in Section 4.3) is a relatively more complex problem representing a simpler version of a real-world
324 problem, which is to design the cross-sectional area of a three-bar truss [55]. This example is presented
325 to demonstrate the superior accuracy of the proposed RBDO method regardless of the desired
326 reliability level. The last problem (in Section 4.4) is to design a three-dimensional multistorey steel
327 structure. Its complexity resembles real-life design, which generally suffers from a lengthy simulation
328 time and where a closed-form analytic solution is unavailable.

329 Note that, prior to employing RBDO, one could perform sensitivity analysis using methods such
330 as principal component analysis [69] to study the influence variables have on performance functions,
331 and potentially consider reducing their dimensions if necessary. However, the paper rather focuses on
332 the reliability analysis of performance functions (with or without reduced dimensionality).

333 4.1. Highly nonlinear numerical problem

334 4.1.1. Problem formulation

335 The objective of this optimisation problem, which is mathematically represented as:

$$\text{Find} \quad : \quad \mu_{X_1} \text{ and } \mu_{X_1} \quad (6)$$

Minimise : $f(\mu_{X_1}, \mu_{X_2}) = \mu_{X_1} + \mu_{X_2}$
 Subject to : $g(\mathbf{X}) \leq 0$
 Where : $\{0,0\} \leq \mathbf{d} \leq \{4,4\}$ and $\sigma_{\mathbf{X}} = \{0.3,0.3\}$

336 is to find the mean of random variables $\mathbf{X} = \{X_1, X_2\}$ with the relationship $\mathbf{d} = E[\mathbf{X}] = \{\mu_{X_1}, \mu_{X_2}\}$ such
 337 that the objective function $f(\cdot)$ is minimised. In this problem, two different versions of highly
 338 nonlinear constraint function $g(\cdot)$ are used. They are given in the form:

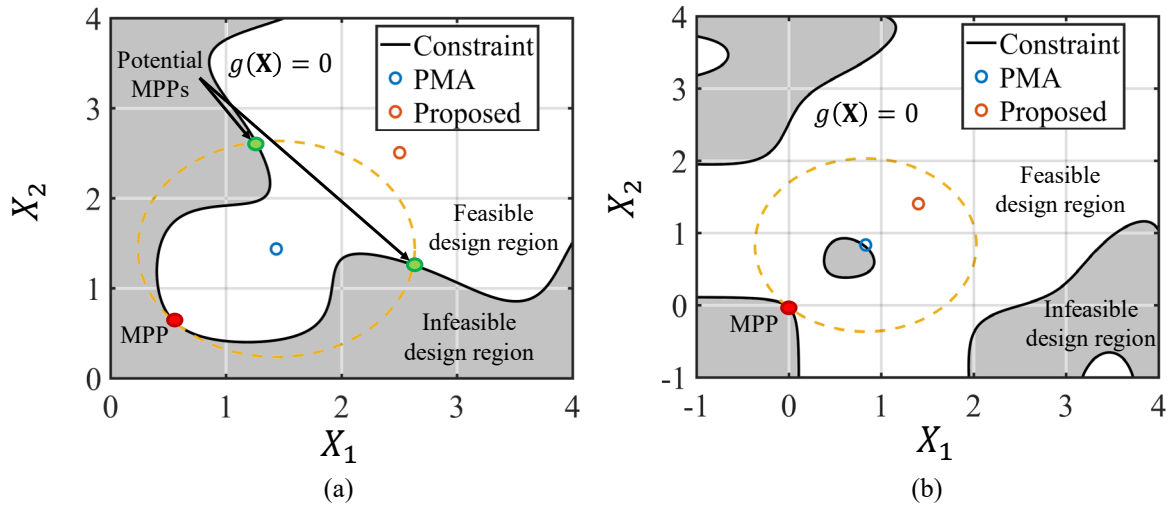
$$g(\mathbf{X}) = \sum_{ij} a_{ij} X_1^i X_2^j, \quad (7)$$

339 whereby the constant a_{ij} are provided in Table 1 to keep the section succinct. These constraint
 340 functions are graphically illustrated in Figure 3(a) and (b) respectively. The shaded regions in Figure
 341 3 reflect the infeasible region which do not meet the constraint $g(\cdot) \leq 0$ as formulated in (6). In other
 342 words, the design point should not fall in the shaded region. The target reliability index used in this
 343 problem is $\beta = 4$, which translates to 99.9968% reliability, and random variables X_1 and X_2 follow
 344 the normal distribution with the standard deviation 0.3. All RBDO methods start from point $\mathbf{d} =$
 345 $\{3.00, 3.00\}$.

346 Table 1. List of constants a_{ij} for the random variables X_1 and X_2 in (7) for two versions of constraint functions (a) and (b).

a_{ij}		X_1^i						
		Constraint function (a)						
X_2^j	i	0	1	2	3	4	5	
	0	-0.4535	0.0146	-0.4300	0.4347	-0.137	0.0139	
	1	0.0146	1.0975	3.3781	-3.6907	1.1775	-0.1208	
	2	-0.4300	3.3781	-8.9281	6.1153	-1.5913	0.1423	
	3	0.4347	-3.6907	6.1153	-3.3288	0.7266	-0.0550	
	4	-0.1370	1.1775	-1.5913	0.7266	-0.1295	0.0073	
	5	0.0139	-0.1208	0.1423	-0.0550	0.0073	-0.0001	
Constraint function (b)								
0	0.0298	0.7964	-0.6963	0.1998	-0.0201	-		

1	0.7964	-6.8989	7.1431	-2.4586	0.2749	-
2	-0.6963	7.1431	-7.2689	2.4965	-0.2799	-
3	0.1998	-2.4586	2.4965	-0.8554	0.0959	-
4	-0.0201	0.2749	-0.2799	0.0959	-0.0107	-
5	-	-	-	-	-	-



347

348
349
350
351

Figure 3. Surface regions constructed in the RBDO method for the problem (6) where (a) and (b) show different versions of the highly nonlinear performance function (7) where their constant values are listed in Table 1. The final designs are obtained using the PMA and moment-based RBDO methods which are illustrated in blue and red circles respectively. The dashed yellow lines represent circles with radius β of 4 around the PMA design points in order to find all potential MPPs, which are in solid points.

352

The goal of this example is to demonstrate the fundamental limitations of sampling methods (e.g.,

353

MC and IS methods) and MPP-based RBDO methodologies. These limitations are inherent within the

354

basic assumptions of these methods that are not easily addressable. The *performance measure*

355

approach (PMA), which has been shown to possess superior accuracy compared to other MPP-based

356

strategies [10], is used in this section to represent MPP-based methods. The gradient information

357

required by the MC method (which uses 10^6 independent realisations) for updating design points has

358

been calculated using the expression recommended by its proponents [11]. The performance functions

359

$g(\cdot)$ are bivariate polynomials (7); eliminating any potential uncertainty that arises from modelling. In

360

other words, this example focuses on the reliability estimation; hence, Step 2 and selective sampling

361

in the flowchart Figure 1 has been omitted.

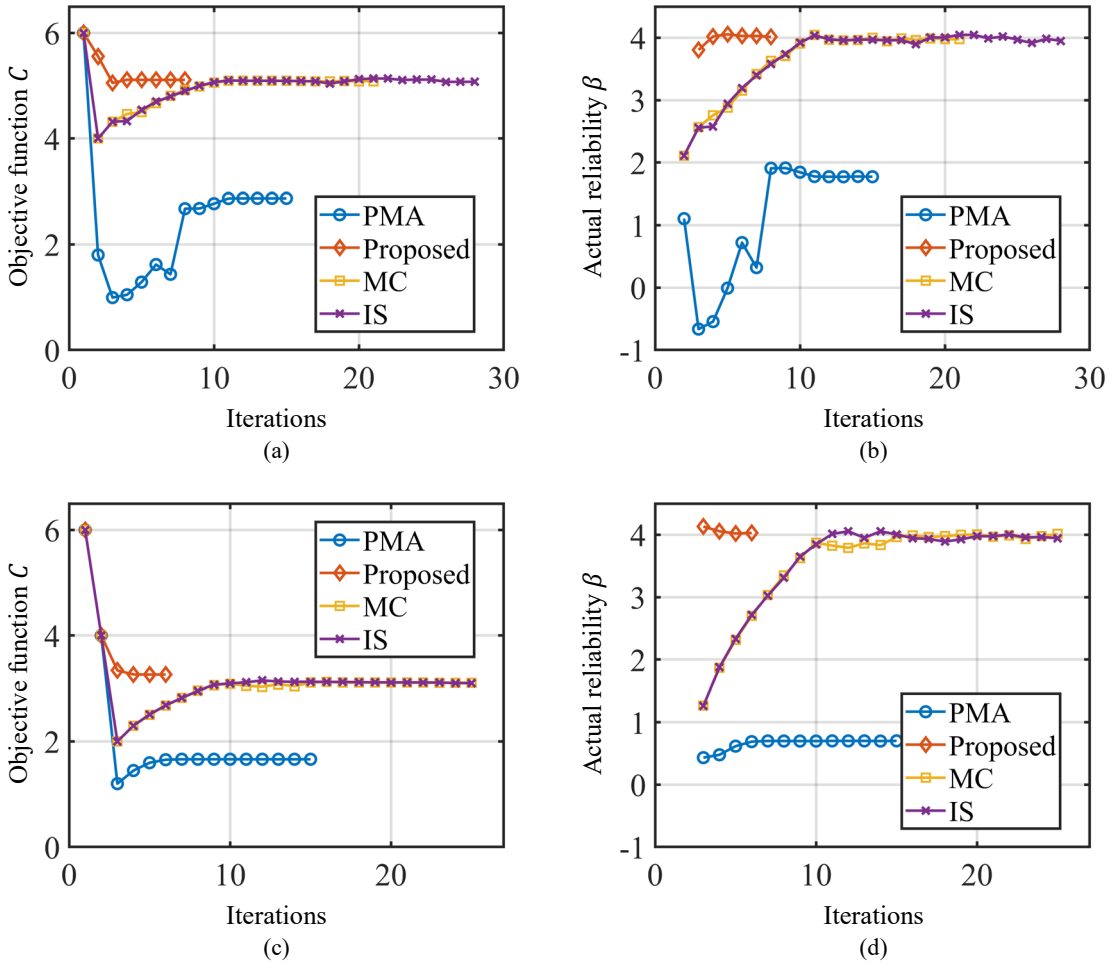
362 4.1.2. Results

363 The performance metric of this optimisation problem is the accuracy of the estimated reliability
 364 corresponding to the respective designs. They are calculated using MC method with 10^8 independent
 365 realisations, whereby the actual reliability β has been estimated to a standard uncertainty of less than
 366 10^{-4} , about 1% of the observed gap between the achieved and targeted β ; hence, making the reported
 367 difference of β values statistically significant. In the event of mismatch between design reliability and
 368 the targeted reliability, over-design where higher-than-target final reliability value is preferred over
 369 under-design. Table 2 presents the results of the PMA, proposed moment method and MC methods.
 370 The final design points obtained from the PMA and the proposed methods are illustrated in Figure 3
 371 in the blue and red circles respectively. The circles with dashed lines are of radius $\beta = 4$ drawn around
 372 the PMA design to show the MPPs. Figure 4 however illustrates the iteration history (objective
 373 function and actual reliability) of both the constraint functions.

374 Table 2. Performance of RBDO methods for highly nonlinear numerical example (6) with the desired reliability $\beta = 4$.

	Design			Actual reliability β
	μ_1	μ_2	C	
Performance function (a)				
PMA	1.4359	1.4359	2.8718	1.7730
MC*	2.5432 (0.0176)	2.5341 (0.0136)	5.0772 (0.0075)	3.9324 (0.0153)
IS*	2.5428 (0.0152)	2.5347 (0.0169)	5.0779 (0.0067)	3.9332 (0.0184)
Proposed	2.5555	2.5555	5.1110	4.0089
Performance function (b)				
PMA	0.8314	0.8314	1.6628	0.7000
MC*	1.5934 (0.0421)	1.5940 (0.0419)	3.1975 (0.0129)	3.9977 (0.0263)
IS*	1.5899 (0.0502)	1.5952 (0.0397)	3.1989 (0.0133)	3.9992 (0.0285)
Proposed	1.6307	1.6307	3.2613	4.0257

375 *Did not converge. Results indicate the mean and standard deviation (in parentheses)
 376 calculated from 10 runs.



377
378
379
380

Figure 4. Plots (a) and (b) show the convergence of the objective function C and actual reliability β of example (a) respectively whereas plots (c) and (d) show those of example (b). The four distinct lines represent the results of the PMA, proposed, MC, and IS methods respectively.

381 *4.1.3. Discussion*

382 The results from Table 2 show that PMA converges to a solution that has incredibly low reliability.
383 In the example (a), instead of the targeted 99.9968% reliability ($\beta = 4$), PMA design only achieved
384 96.1886% reliability ($\beta = 1.773$). In example (b), not only is the design much less reliable at
385 75.8036%, the final design itself is sitting on the forbidden region. In other words, PMA design will
386 fail the design feasibility requirements even when all parameters have zero variance. The failure of
387 PMA design to achieve the target reliability means that the method has failed the primary mission of
388 RBDO. These observations are consistent with studies [36] where the severity of underestimation
389 increases with the nonlinearity of the performance functions. This is primarily due to the reliability
390 approximation strategy hinging on MPP.

391 For instance, the dashed circles in Figure 3(a) and (b) represent radius $\beta = 4$. The corresponding
392 MPPs, which are the intersection points between $g(\cdot) = 0$ and the dashed circles, can also be observed.
393 Figure 3(a) shows that the MPP is not unique in the reliability analysis by the PMA. More importantly,
394 the infeasible design region inside the circle has not been taken into account, severely affected the
395 reliability estimation. This is caused by the reformulation of the original problem into an MPP form.
396 The reformulated optimisation problem will try to keep the design point at a specified distance of $\beta =$
397 4 from the MPP. This single-pointed focus on a MPP, instead of going through nested integral of all
398 points in the vicinity of the design point, is the main reason MPP-based method can achieve high speed
399 computation; but it also blinds the algorithm to the surrounding reliability landscape such as other
400 MPPs and nearby infeasible design regions. This result shows that MPP-based methods are only
401 reliable when the admissible region exhibits sufficient continuity and convexity that matches the
402 assumption in the formulation. More often than not, it is difficult to guarantee that the required
403 continuity and convexity conditions can be satisfied by a complex system near the edge of its reliability
404 limit.

405 Table 2 also shows that MC/IS output results in the vicinity of the actual solution, but the optimiser
406 does not converge because the solution fluctuation is larger than the specified tolerance. The iteration
407 history illustrated in Figure 4 show that MC and IS behave in a very similar fashion even though IS is
408 known to be more sample-efficient compared to MC. The observational summary of many MC/IS runs
409 is that, the primary challenge is not the sampling efficiency. Instead, the sensitivity of the convergence
410 with respect to sampling noise is the main difficulty. As the solution approaches the optimal point, the
411 gradient approaches zero, and small perturbations arising from the MC/IS sampling noise can end up
412 dominating the direction of the optimisation thus pulling the optimiser away from the true solution.
413 Hence, the solution will bounce around the true solution without convergence until the optimiser
414 terminates by external conditions, e.g. maximum iteration limit, or fortuitously satisfy one of many
415 termination conditions. Increasing the sample size reduces the variance of the solutions, however this

416 will not fundamentally resolve the problem. It is important to note that the sample size grows quickly
417 with respect to the variance reduction (sample size is in the order that is reciprocal to the variance in
418 MC). This observation may explain why existing RBDO problems that use direct sampling methods
419 for reliability analysis, such as in [12, 70], have confined their designs to very low target reliability of
420 $\beta = 2$. The sampling noise in MC/IS can also cause inconsistent constraint satisfaction which
421 sometimes causes abnormal early termination of the optimisation [24].

422 One possible way of overcoming this shortcoming is by increasing the termination tolerances. As
423 examples, the results of the MC and IS methods in Table 2 were obtained using constraint, optimality,
424 and step tolerances of 1×10^{-6} (see MATLAB documentation [56] for tolerances information). From
425 100 trials, it was found that, for performance function (a), the probability of convergence is 0.79 with
426 standard deviation of 0.0179. When the tolerance values were increased to 1×10^{-4} , the probability
427 of convergence increased to 0.98 with a larger standard deviation of 0.0510. Similar observations were
428 also made with performance function (b). Two deductions can be made from these results. First, using
429 the MC method for reliability analysis introduces uncertainty and complications of problem-specific
430 tuning into the optimiser convergence. One needs to run the simulation many rounds in order to find
431 the average final design. However, running multiple simulations defeats the purpose developing
432 efficient sampling techniques for response surface modelling, such as in [11, 12]. Second, although
433 the convergence can be guaranteed with a “looser” optimiser termination tolerance, it comes at the cost
434 of larger variance in the reliability estimation, which in turn, requires more repetitions. Therefore, in
435 light of the results presented here, MC method is not recommended for design optimisation when high
436 reliability design is sought. Furthermore, due to the uncertainty in the optimiser convergence, the MC
437 method will not be employed for reliability analysis in the following problems.

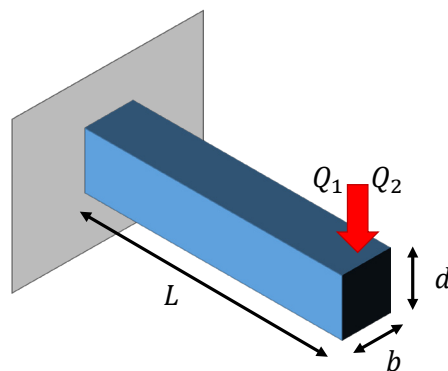
438 On the other hand, such problems are not observed in the moment method. When the moments
439 and the corresponding distributions are accurately computed, the RBDO converges to a design
440 satisfying the target reliability of $\beta = 4$. The robustness of the moment method in comparison to the

441 MC and MPP-based methods shown in the problem makes it the desirable candidate for reliability
442 analysis in RBDO. Normally, modelling uncertainty (if metamodeling is employed) and reliability
443 calculation method are two sources of reliability estimation error in RBDO. It can be inferred from the
444 results in Table 2 that, the moment method could potentially render errors from the reliability
445 calculation method such that it is insignificant in comparison with modelling uncertainty. Therefore,
446 the adoption of the moment method in RBDO will also reduce the convolution of these two sources of
447 error and facilitate transparent comparison by shifting the focus to modelling accuracy and efficiency.

448 4.2. Cantilever beam

449 4.2.1. Problem formulation

450 This example is one of the most commonly used benchmark problems [55, 68] to assess the
451 performance of different RBDO methods. In this example, the proposed method in Figure 1 will be
452 employed without omitting any of the steps. Here, a simple cantilever beam with breadth b and depth
453 d , as illustrated in Figure 5 will be optimised. The objective is to design the lightest cantilever while
454 observing the performance function constrains describing various failure modes. The performance
455 functions are given in (8), and they are: 1) failure by buckling; 2) fatigue; 3) excessive deflection; and
456 4) stress, respectively. The details of the variables in problem (8) and their respective statistical
457 properties are outlined in Table 3. The starting point used for the RBDO problem is $\{b, d\} = \{2.0, 2.0\}$.
458 The target reliability index $\beta_{1,2}$ is 3 for g_1 and g_2 , and $\beta_{3,4}$ is 2 for g_3 and g_4 .



459

460 Figure 5. Illustration of the cantilever beam problem. Symbols b , d , L , Q_1 , and Q_2 denote the breadth, depth, length, fatigue load, and
461 design load of the cantilever beam respectively.

Find : b and d

Minimise : $f(b, d) = bd$

Subject to : $g_1 = Q_2 - \frac{0.3Eb^3d}{L^2} \leq 0$ $g_2 = N_0 - A \frac{6Q_1L}{bd^2} \leq 0$ (8)

$g_3 = \frac{4Q_2L^3}{Ebd^3} - \Delta_0 \leq 0$ $g_4 = \frac{6Q_2L}{bd^2} - R \leq 0$

Where : $L = 30$ in. $N_0 = 2 \times 10^6$ cycles $\Delta_0 = 0.15$ in. $\beta_{1,2} = 3$ and $\beta_{3,4} = 2$

462 Table 3. Properties of the random variables for the cantilever beam example, whereby CoV denotes the coefficient of variation.

Symbols	Description	Distribution	Mean (* for median)	CoV
Q_1	Fatigue load (lbs)	Lognormal	0.4*	0.15
Q_2	Design load (lbs)	Lognormal	0.5*	0.15
E	Young's modulus (ksi)	Normal	30000.0	0.10
A	Fatigue strength coefficient (ksi)	Lognormal	1.46e10*	0.50
R	Yield strength (ksi)	Weibull	50.0	0.12

463 4.2.2. Results

464 Table 4 and Table 5 present the results of the RBDO methods and the iteration history of the
465 proposed moment-based RBDO method respectively. The function evaluations reported in Table 4 is
466 the number of times the performance functions g_{1-4} were evaluated throughout the optimisation
467 procedure. The difference in the number has a significant impact on the overall computational time
468 since the finite element computation of complex structural models (for function evaluation) is the most
469 time-consuming part of reliability estimation. Therefore, the number of function evaluations is used as
470 a measure of the computational efficiency, whereby a smaller number indicates a higher efficiency.
471 Note that the benchmark results are variations of MPP-based methods and are extracted directly from
472 the number of iterations when SQP optimiser is employed [55]. The values in the parentheses,
473 however, is the number of additional function evaluations required using FDM to calculate sensitivity.
474 FDM typically requires additional function evaluations equivalent to the number of design variables.
475 However, note that the primary focus of discussion in the current and upcoming examples is the
476 accuracy of meeting the target reliability index. Similar to the previous experiment, the actual
477 reliability index of the final design, denoted by β in Table 4, is calculated using MC simulation with

478 10^8 samples of random realisations, whereby a higher but closer value to the target reliability β is
 479 desired (i.e. 3 for g_1 and g_2 , and 2 for g_3 and g_4).

480 Table 4. RBDO results of the cantilever design problem. The most probable failure point (MPFP) and the minimum performance target
 481 point (MPTP) methods are both MPP-based techniques [55]. The values in parentheses represents the function evaluations to calculate
 482 the first-order derivative method for sensitivity analysis.

Methods	Final design			Function evaluations				β				
	b	d	f	g_1	g_2	g_3	g_4	Total	g_1	g_2	g_3	g_4
Deterministic	0.2383	3.6925	0.8801					30	-	-	-	-
MPFP [55]				94 (188)	187 (394)	85 (170)	104 (208)	1430				
MPTP [55]	0.2806	3.9516	1.1088	61 (122)	33 (66)	77 (154)	74 (148)	735	2.9763	Inf	1.9780	3.4811
Proposed	0.2810	3.9551	1.1113	2 (4+1) (4*2+1) = 90				30 + 90 = 120	3.0039	Inf	2.0003	3.4905

483 Table 5. Iteration history of the proposed moment-based RBDO method for the cantilever beam example.

Iteration	Design			Function evaluations			
	b	d	f	g_1	g_2	g_3	g_4
0	2.0000	2.0000	4.0000				3
1	1.3357	1.9992	2.6703				6
2	0.8216	2.3294	1.9138				9
3	0.5116	2.7269	1.3950				12
4	0.3374	3.1597	1.0659				15
5	0.2582	3.5260	0.9104				18
6	0.2393	3.6787	0.8803				21
7	0.2384	3.6924	0.8801				24
8	0.2384	3.6925	0.8801				27
9	0.2384	3.6925	0.8801				30
10	0.2384	3.6925	0.8801				75
11	0.2951	3.7175	1.0969				
12	0.2809	3.9485	1.1091				120
13	0.2810	3.9551	1.1113				
	0.2810	3.9551	1.1113				

484 4.2.3. Discussion

485 It can be observed from Table 4 that all the RBDO methods, i.e., the MPP-based (MPFP and
 486 MPTP) and the proposed algorithms converge. Although the MPTP is the computationally more

487 efficient MPP-based method in this example, it still requires approximately six times more function
488 evaluations compared to the proposed method.

489 Table 5 shows that such a boost in the computation efficiency is achievable due to the employment
490 of a metamodel approach instead of the performance functions when calculating reliability. In the
491 proposed method, the response surface is modelled only twice after the deterministic optimisation. A
492 new response surface was not built after iteration 11 since the boundary region did not exceed the
493 surface region in the selective sampling technique. Furthermore, unlike the MPP-based methods, the
494 proposed method shares the same design points to construct the response surface models for all four
495 performance functions simultaneously and therefore, they share the function evaluation number.
496 Consequently, the total number of performance function evaluations can be significantly reduced. As
497 a result, the computational efficiency in finding the localised response surface models in the RBDO is
498 significantly improved, which is one of the notable highlights of using response surfaces in the
499 proposed method. Nevertheless, note that the proposed method does not claim full credit for the
500 improved computational efficiency as this can also be achieved for MPP-based methods by employing
501 the same metamodeling and sampling techniques or other more efficient localised response surface
502 modelling methods such as [11, 12].

503 Table 4 goes on to show that the proposed moment-based method is more reliable than the MPP-
504 based methods. The MPP-based methods arrived at designs that are lighter (smaller cross-sectional
505 area) but violates the reliability requirements of g_1 and g_3 . Some existing works, such as [55], did not
506 perform design validation through MC simulation; and the validation of the actual β in Table 4 reveal
507 the importance of doing so. It can be seen that the MPP-based designs have failed to satisfy the
508 prescribed reliability requirement due to lower precision in the reliability calculation. The standard
509 deviation of MC at 10^8 samples for β_1 and β_3 are 2.5×10^{-3} and 9.0×10^{-4} , respectively, which are only
510 less than 10% of the observed gap between the achieved and targeted $\beta_{1,3}$. Therefore, the observed
511 under-design is statistically significant. In agreement with literature [36], the error in the reliability

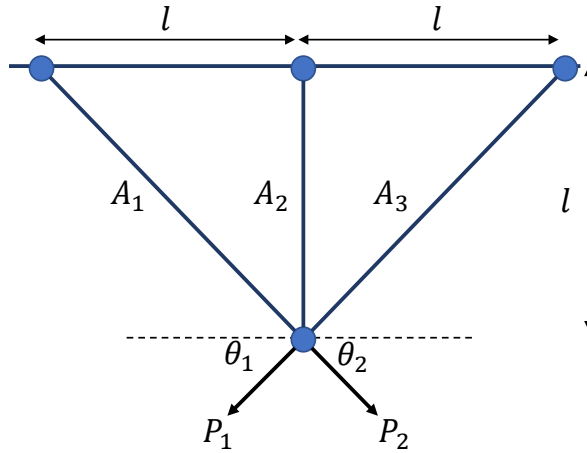
512 estimation is inherent in the MPP-based approximation and the normalisation transformation of
513 random variables required by MPFP and MPTP. The occurrence of under-design in the mainstream
514 MPP-based methods for a simple cantilever system is a cause of concern for potential users working
515 on safety critical systems. This cannot be addressed even with the use of effective response surface
516 modelling techniques because of the implicit assumptions within the MPP transformation and
517 approximation schemes.

518 On the contrary, this is not the case with the proposed method due to the high modelling accuracy
519 of the polynomial genetic programming, the precise analytical moments, and the robust moment-
520 constrained maximum entropy method integrated into the proposed moment-based RBDO framework.

521 4.3. Three-bar truss

522 4.3.1. *Problem formulation*

523 This example is in accordance to [55], whereby the cross-sectional area of a three-bar truss, as
524 shown in Figure 6, is minimised. This problem is more complex than the cantilever model, but still
525 admits a closed-form solution for benchmarking purposes [71]. The performance functions are the
526 stress constraints as shown in (9). As the problem is symmetrical, A_1 and A_3 are treated as one
527 variable. The starting point of the optimisation is $\{A_1, A_2\} = \{0.85, 2.00\}$ and the RBDO problem is
528 performed twice for $\beta_{1,2} = 2$ and $\beta_{1,2} = 3$. The ANSYS software is used for FEM and to consequently
529 model the response surfaces of g_1 and g_2 using the polynomial genetic programming. Table 6 presents
530 the details of the variable notations and their statistical properties respectively.



531

532
533

Figure 6. Illustration of the three-bar truss problem. Symbols A_1 , A_2 , and A_3 denote the cross-sectional area of the bars respectively, θ_1 and θ_2 denote the loading angles of loads P_1 and P_2 respectively, and l denotes the nodal distance.

Find : A_1 and A_2

Minimise : $f(A_1, A_2) = 2\sqrt{2}A_1 + A_2$ (9)

Subject to : $g_i = \sigma_i - \sigma^+ \leq 0 \quad i = 1, 2$

Where : $l = 10$ in. $A_1 = A_3 \quad \{0.5, 0.0\} \leq \{A_1, A_2\} \leq \{1.2, 4.0\} \quad \beta_{1,2} = 2$ and $\beta_{1,2} = 3$

534
535

Table 6. Properties of the deterministic and random variables for the three-bar truss example, whereby CoV denotes the coefficient of variation.

Symbols	Type	Description	Distribution	Mean (* for median)	CoV
A_1	Deterministic	Cross-sectional area bar 1 (in. ²)		Not applicable	
A_2		Cross-sectional area bar 2 (in. ²)			
P_1	Random	External load (lbs)	Gumbel	20000	0.20
P_2		External load (lbs)	Gumbel	20000	0.20
θ_1		Loading angle (rad)	Normal	$\pi/4$	0.10
θ_2		Loading angle (rad)	Normal	$\pi/4$	0.10
σ^+		Allowable tensile stress (psi)	Lognormal	20000*	0.05

536

4.3.2. Results

537

Table 7 presents the results of the RBDO problem for both $\beta_{1,2} = 2$ and $\beta_{1,2} = 3$. The accuracy

538

of the reliability constraints in Table 7 is calculated using MC simulation with 10^8 samples of random

539

realisations using the closed-form expressions of the performance functions given in [71]. Similar to

540

the previous problem, the performance metrics for this example are the number of function evaluations

541

and the reliability index of the final design.

542
543
544

Table 7. RBDO results of the three-bar truss problem for $\beta_{1,2} = 2$ and $\beta_{1,2} = 3$. The most probable failure point (MPFP) and the minimum performance target point (MPTP) methods are both MPP-based techniques [55]. The values in parentheses represents the function evaluations to calculate the first-order derivative method for sensitivity analysis.

Methods	Final design			Function evaluations			β	
	$A_1 = A_3$	A_2	f	g_1	g_2	Total	g_1	g_2
$\beta_{1,2} = 2$								
Deterministic	0.6363	1.2726	3.0723	20		20	-	-
MPFP [55]	0.5613	1.5005	3.0882	49 (98)	42 (84)	273	2.0286	1.8723
MPTP [55]	0.5618	1.5002	3.0892	65 (130)	50 (100)	345	2.0299	1.8728
Proposed	0.5765	1.5364	3.1669	4 (2+1) (2*7+1) = 180		20 + 180 = 200	2.0889	2.0061
$\beta_{1,2} = 3$								
Deterministic	0.6363	1.2726	3.0723	20		20	-	-
MPFP [55]	0.9694	1.5952	4.3371	63 (126)	47 (94)	330	3.0287	2.8571
MPTP [55]	0.9706	1.5942	4.3403	48 (96)	40 (80)	264	3.0293	2.8556
Proposed	0.9523	1.7042	4.3977	4 (2+1) (2*7+1) = 180		20 + 180 = 200	3.0489	3.0714

545 4.3.3. Discussion

546 Table 7 shows that, for the three-bar truss problem, the proposed moment-based RBDO method is
547 more accurate and computationally more efficient than the MPP-based methods regardless of the target
548 reliability indexes $\beta_{1,2}$. Unlike the MPFP and MPTP, the reliability index of the proposed RBDO
549 design meets the target reliability index requirement for all performance functions. The advantageous
550 accuracy in the reliability index shown by the proposed method in the previous example is also
551 observed in this more complex multi-component system. The main contributing factor for such
552 accuracy is the analytical MUET accompanied by the robust maximum entropy algorithm that can
553 accurately approximate the “tail” of the probability distribution utilising the information contained in
554 the high-order moments.

555 The cross-sectional area of the proposed method is higher than both MPFP and MPTP; however,
556 the target reliability index for both the performance functions are met; thus, guaranteeing the accuracy
557 of the proposed framework. Although the proposed method does not give the computational boost of
558 the magnitude observed in the cantilever beam example, its number of function evaluations is still
559 lower than that of the MPP-based methods. This is due to the selective sampling method in the local
560 response surface modelling. More importantly, this computational efficiency is achieved with no

561 compromise in the accuracy of the reliability analysis; hence suggesting that MPFP and MPTP
562 methods can also benefit from using localised metamodels for reliability analysis. However, it will not
563 address the inaccurate reliability index achieved by employing those MPP-based methods.

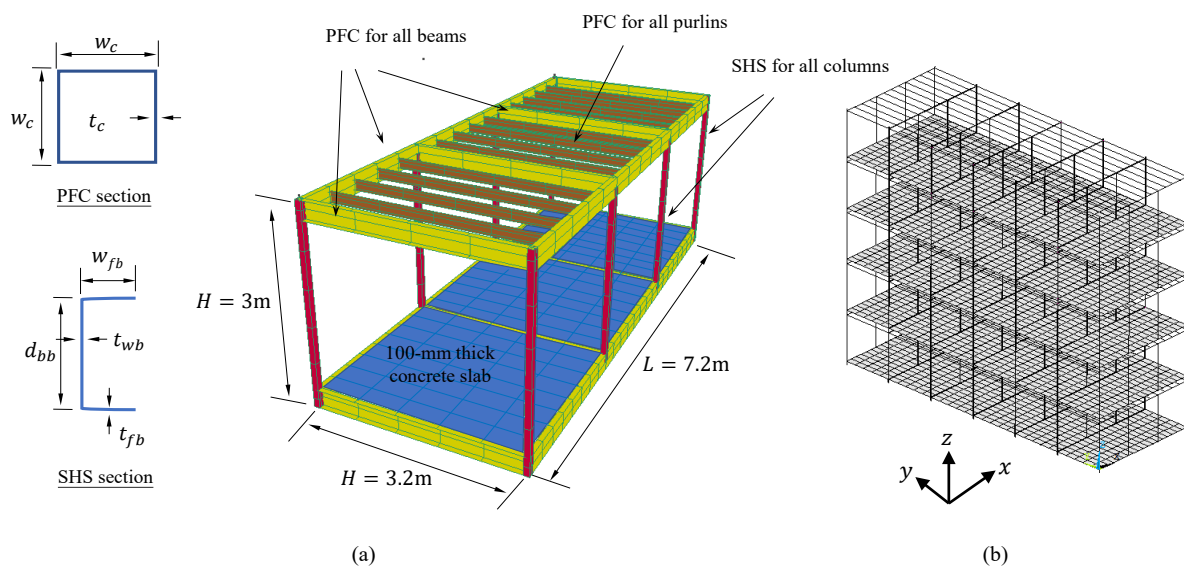
564 Both benchmark problems show that the proposed moment-based RBDO method is more effective
565 than the MPP-based methods. Although the presented work does not claim full credit for the
566 improvement in computational efficiency, the combination of better accuracy and higher
567 computational efficiency of the proposed RBDO method is essential for the design of complex
568 structures where one execution of finite element model could take hours, or even days, to complete.
569 One such structure is therefore used in the following example to exhibit the applicability of the
570 proposed method.

571 4.4. Three-dimensional multistorey structure

572 4.4.1. *Problem formulation*

573 Figure 7 shows the FE model of a three-dimensional steel framed modular building as an example
574 of a relatively complex structure. The structure is a five-storey building assembled with steel-framed
575 modules. Each storey consisted of 6 identical corner-supported modules with the length of 7.2 m, width
576 of 3.2 m and height of 3.0 m. The cross-sections for the framing members were assumed to be parallel-
577 flange channel sections for all beams and purlins, and square hollow sections for all columns. The
578 cross-section shapes are also indicated in Figure 7 (a). The floors were concrete slabs with a thickness
579 of 100 mm. All inter-module connections were assumed ideally pinned connections. The uncertainties
580 (or randomness) in steel-framed modular buildings often arise from the prefabricated steel modules
581 with a combination of standardised parameters. It is, therefore, imperative to consider the overall
582 structural reliability from putting together numerous modules to form a complex structural frame, and
583 this is when the computational efficiency and accuracy of the proposed method can be invaluable to
584 the engineers.

585 The FE model in Figure 7 was created based on the modelling techniques outlined in [72-74]. In
 586 this study, the structure is subjected to combination of dead load (including self-weight and
 587 superimposed dead load), live load and wind load. The dead load due to self-weight was generated
 588 using gravity field in ANSYS. The design wind direction is assumed parallel to the global x -direction
 589 as indicated in Figure 7. The windward, leeward and roof wind pressures were determined based on
 590 the suggested wind speed for Cyclonic Region C as per AS1170.2 [75] by the *Standards Association*
 591 *of Australia* (SAA).



592

593 Figure 7. Illustration of the three-dimensional multistorey structure where (a) is the single volumetric module and (b) is the full
 594 structure model. Here, in this paper, purlins and beams are assumed to have the same sectional dimension.

595 As shown in formulation (10), the structure is optimised by minimising the total volume of the
 596 columns and beams, which in turn minimises the structural self-weight. Three performance functions
 597 were chosen, including: 1) inter-storey drift under SLS loading as per AS1170.0 [76], 2) ULS
 598 performance of columns subjected to combined axial (N_x^*) and flexural actions (M_y^* and M_z^*) as per
 599 AS4100 [19]; 3) ULS performance of beams as per AS4100 [77] by the SAA. The structure is deemed
 600 to have failed when any one of the above performance functions is not satisfied. The target reliability
 601 index is that $\beta_1 = 3$ for g_1 , and $\beta_{2,3} = 3.8$ for g_2 and g_3 as suggested in *International Organization*
 602 *for Standardization* (ISO) 13822 [78].

603 Here, M_{cx} and M_{cy} are the member moment capacities with respect to the principle and minor axes
604 respectively. N_{cx} is the column capacity. Z_{be} and Z_{ce} are the section modules for beams and columns
605 respectively, A_c and A_b are the cross-sectional area for beams and columns respectively. These
606 properties can be determined based on the geometric and material properties given in Table 8. The
607 probabilistic models for load variables were determined according to *Australian Building Codes Board*
608 (ABCB) Handbook [79] and the material models were determined according to *Joint Committee on*
609 *Structural Safety* (JCSS) code [80]. Table 8 summaries the properties of random variables for the three-
610 dimensional multistorey structure problem. The starting point of the optimisation is that
611 $\{w_c, t_c, w_{fb}, d_{bb}, t_{fb}, t_{wb}\} = \{100, 9.0, 133, 202, 7.0, 5.0\}$ mm.

Find : $w_c, t_c, w_{fb}, d_{bb}, t_{fb}$ and t_{wb}

Minimise : $f = \sum L_c A_c + \sum L_b A_b$

Subject to :

$$g_2 = \left(\frac{M_y^*}{M_{cy}}\right)^{1.4} + \left(\frac{M_z^*}{M_{cz}}\right)^{1.4} \leq 1,$$

$$g_1 = \Delta - H/500 \leq 0$$

whereby $M_{ci} = M_{cs} \left(1 - \frac{N_x^*}{N_{cx}}\right)$ for $i = x, y$, $N_{cx} = \alpha_c A_c f_y$ and $M_{cs} = Z_{ce} f_y$ (10)

$$g_3 = \alpha_m \alpha_s M_{bs}, \text{ whereby } M_{bs} = Z_{be} f_y$$

Where : $\alpha_m = 1.0$ $H = 3$ m $\sum L_c = 720$ $\sum L_b = 1248$ $\beta_1 = 3$, and $\beta_{2,3} = 3.8$

612 Table 8. Properties of the random variables for the three-dimensional multistorey structure problem, whereby CoV denotes the
613 coefficient of variation.

	Description	Distribution	Median		CoV
			SLS	ULS	
<i>SIDL</i>	Superimposed dead load (Pa)	Lognormal	1000		0.10
<i>LL</i>	Live load (Pa)	Lognormal	1500		0.43
w_c	Width of column (Pa)	Normal			0.0205
t_c	Wall thickness of column (Pa)	Normal			0.0362
w_{fb}	Flange width of beam (Pa)	Normal			0.0132
d_{bb}	Depth of beam (Pa)	Normal	Not applicable		0.0364
t_{fb}	Flange thickness of beam (Pa)	Normal			0.0182
t_{wb}	Web thickness of beam (Pa)	Normal			0.0151
E_s	Elastic modulus of steel (Pa)	Lognormal	206×10 ⁹		0.03
E_c	Elastic modulus of concrete (Pa)	Lognormal	21.8×10 ⁹		0.15

p_W	Windward wind pressure (Pa)	Lognormal	169.5040	432.0960	0.16
p_L	Leeward wind pressure (Pa)	Lognormal	56.4987	144.0309	0.16
p_R	Roof wind pressure (Pa)	Lognormal	169.4961	432.0927	0.16
Rou_S	Density of steel (kg/m ³)	Lognormal	7700		0.01
Rou_C	Density of concrete (kg/m ³)	Lognormal	2400		0.04
f_y	Yield stress of steel (Pa)	Lognormal	350×10 ⁶		0.05

614 4.4.2. Results

615 Table 9 presents the RBDO problem results, where MPP-based RBDO using FORM [33] is also
616 employed for benchmarking the results of the proposed method. Like the previous examples, the
617 reliability index of the final RBDO designs is reported in Table 9 using MC simulation with the data
618 obtained from the ANSYS model of the structure in Figure 7; however, only the final reliability index
619 of the performance function g_1 is presented in Table 9 as the reliability index of both g_2 and g_3 are
620 infinity, implying that g_1 is the only active constraint that determines the final design.

621 Table 9. RBDO results of the three-dimensional multistorey structure problem. The reliability index of g_2 and g_3 is infinity. The
622 FORM was employed using the state-of-the-art MPP-based algorithm provided in [33].

Methods	Final design							Function evaluations			β	
	w_c	t_c	w_{fb}	d_{bb}	t_{fb}	t_{wb}	f	g_1	g_2	g_3	Total	g_1
Deterministic	0.0947	0.0050	0.0750	0.2300	0.0120	0.0060	5.0801		120		120	-
FORM [33]	0.0988	0.0050	0.0750	0.2300	0.0120	0.0060	5.1828	2170	1798	2054	6022	2.8043
Proposed	0.0976	0.0050	0.0750	0.2300	0.0120	0.0060	5.2000		3(3+1) (2*17+1) = 420		540	3.0274

623 4.4.3. Discussion

624 Table 9 shows that, for the RBDO of the complex steel structure in Figure 7, a total of 6022
625 evaluations are required for the FORM, whereas only 540 evaluations are needed using the proposed
626 moment-based method. Although both the proposed and MPP-based methods converge to respective
627 solutions, it is evident from the results that the proposed method demands significantly fewer function
628 evaluations (approximately 11-fold increase in computational efficiency) due to the use of
629 metamodeling and efficient sampling. More importantly, as in the previous benchmark problems,
630 Table 9 shows that the design obtained from the MPP-based RBDO does not meet the target reliability

631 index β_1 of 3 as described in (10); consequently its resultant structure could possibly be under-
632 designed. This is not the case with the proposed method whereby the desired reliability index is
633 achieved.

634 These observations further substantiate the strengths of the proposed method. The near 11-fold
635 computational efficiency improvement comes from the absence of MPP iterations that occur in the
636 effort to find the reliability constraints as well as the boost from the selective sampling paradigm in
637 finding the local response surface models. Meanwhile, the accuracy of meeting the target reliability
638 index is contributed by the accurate response surface modelling, precise moment calculations, and the
639 maximum entropy distribution fitting. It is important to note that the localised response surface with
640 the selective sampling mechanism can also be employed for MPP-based methods to attain a similar
641 computational efficiency; however, the added assumption on top of the MPP transformation and search
642 strategies in FORM (or SORM) could adversely affect its reliability constraint evaluation accuracy.

643 Meeting the building standards and their reliability constraints are crucial in a safety-critical
644 structural design, especially in areas with conditions such as wind and earthquake. Based on the
645 presented results from the three examples with very different design complexity, it is proven that the
646 proposed moment-based RBDO methodology is a more desirable choice over the MPP-based ones.

647 **5. Conclusion**

648 This study introduces a novel moment-based framework for reliability-based design optimisation
649 (RBDO), which integrates recent advancements made in high order analytical moments and parametric
650 distribution fitting for moment-based reliability (or uncertainty) analysis. The novel moment-based
651 reliability analysis method is proposed alongside several other state-of-the-art techniques, namely:
652 response surface modelling using an evolutionary technique of polynomial genetic programming and
653 a selective sampling method in building localised response surfaces. The proposed method overcomes
654 the common shortcomings reported in the widely used reliability analysis techniques for the RBDO of

655 structural systems, such as the most probable point (MPP)-based methods, Monte Carlo (MC) method,
656 importance sampling (IS) method, and the other moment-based approaches.

657 Results from a newly formulated highly nonlinear RBDO problem shows that the moment method
658 is a more dependable approach for reliability analysis in design optimisation compared to the MPP-
659 based methods and sampling techniques such as the MC method. The MPP-based technique converges
660 to an under-designed solution in a highly nonlinear problem. The convergence of the MC and IS
661 methods, on the other hand, is unguaranteed with uncertainties in the reliability estimation. This was
662 not the case in the moment method, where the final design converges to a solution that meets the target
663 reliability.

664 When the proposed moment-based RBDO method was employed on benchmark problems i.e. the
665 cantilever beam and three-bar truss problems, it was found that the method was more accurate than
666 MPP-based methods. Furthermore, because the computational burden is shifted in the localised
667 sampling scheme for polynomial genetic programming, it also required significantly fewer function
668 evaluations, thus showing excellent overall computational efficiency. Consequently, the proposed
669 method was employed in designing a complex three-dimensional five-storey structure that involves 17
670 random variables. The results show that an optimum design was attained with superior accuracy and
671 computational efficiency, thus demonstrating its value in the design of complex structural systems that
672 involves many random and design variables.

673 Thus far, the known limitation of the proposed approach is that only metamodels that conform to
674 general multivariate polynomial forms can be used for local approximation of the functions. Future
675 goal of this work is to extend the theoretical advancements in calculating analytical moments of
676 multivariate polynomials to those of radial basis functions. This will directly extend its coverage of
677 response surface modelling techniques beyond multivariate polynomials, and in turn increase its scope
678 of practical applications.

679 **Acknowledgement**

680 This work was supported by the 2017 Monash University Vice-Chancellor's International
681 Intercampus PhD Mobility Scheme, IEEE Instrumentation and Measurement Society through the 2017
682 Graduate Fellowship, Massey University Research Funding 2017. The second and third authors also
683 acknowledge the support received from industrial partners of Modular Construction Codes Board and
684 the Department of State Development, Business and Innovation, the State of Victoria, Australia
685 through the Manufacturing Productivity Networks program.

686 **References**

- 687 [1] Haldar A, Mahadevan S. Probability, reliability, and statistical methods in engineering design: John Wiley;
688 2000.
- 689 [2] Huh J, Haldar A. A novel risk assessment for complex structural systems. IEEE Transactions on Reliability.
690 2011;60:210-8.
- 691 [3] Wu J-Y. New enriched finite elements with softening plastic hinges for the modeling of localized failure in
692 beams. Computers & Structures. 2013;128:203-18.
- 693 [4] Okasha NM. An improved weighted average simulation approach for solving reliability-based analysis and
694 design optimization problems. Structural Safety. 2016;60:47-55.
- 695 [5] Ganzerli S, Pantelides C, Reaveley L. Performance - based design using structural optimization. Earthquake
696 engineering & structural dynamics. 2000;29:1677-90.
- 697 [6] Huang M, Chan CM, Lou W. Optimal performance-based design of wind sensitive tall buildings considering
698 uncertainties. Computers & structures. 2012;98:7-16.
- 699 [7] Lagaros ND, Gouvelos AT, Papadrakakis M. Innovative seismic design optimization with reliability
700 constraints. Computer Methods in Applied Mechanics and Engineering. 2008;198:28-41.
- 701 [8] Möller O, Foschi RO, Quiroz LM, Rubinstein M. Structural optimization for performance-based design in
702 earthquake engineering: applications of neural networks. Structural Safety. 2009;31:490-9.
- 703 [9] Goswami S, Ghosh S, Chakraborty S. Reliability analysis of structures by iterative improved response
704 surface method. Structural Safety. 2016;60:56-66.
- 705 [10] Aoues Y, Chateaneuf A. Benchmark study of numerical methods for reliability-based design optimization.
706 Structural and multidisciplinary optimization. 2010;41:277-94.
- 707 [11] Chen Z, Qiu H, Gao L, Li X, Li P. A local adaptive sampling method for reliability-based design
708 optimization using Kriging model. Structural and Multidisciplinary Optimization. 2014;49:401-16.
- 709 [12] Li X, Qiu H, Chen Z, Gao L, Shao X. A local Kriging approximation method using MPP for reliability-
710 based design optimization. Computers & Structures. 2016;162:102-15.
- 711 [13] Cheng J, Li Q. Reliability analysis of structures using artificial neural network based genetic algorithms.
712 Computer Methods in Applied Mechanics and Engineering. 2008;197:3742-50.
- 713 [14] Dai H, Zhao W, Wang W, Cao Z. An improved radial basis function network for structural reliability
714 analysis. Journal of mechanical science and technology. 2011;25:2151.
- 715 [15] Hyeon Ju B, Chai Lee B. Reliability-based design optimization using a moment method and a kriging
716 metamodel. Engineering Optimization. 2008;40:421-38.
- 717 [16] Low Y. A new distribution for fitting four moments and its applications to reliability analysis. Structural
718 Safety. 2013;42:12-25.

- 719 [17] Lu Z-H, Cai C-H, Zhao Y-G. Structural Reliability Analysis Including Correlated Random Variables Based
720 on Third-Moment Transformation. *Journal of Structural Engineering*. 2017;143:04017067.
- 721 [18] Lu Z-H, Hu D-Z, Zhao Y-G. Second-Order Fourth-Moment Method for Structural Reliability. *Journal of*
722 *Engineering Mechanics*. 2016;143:06016010.
- 723 [19] Zhang X, Pandey MD. Structural reliability analysis based on the concepts of entropy, fractional moment
724 and dimensional reduction method. *Structural Safety*. 2013;43:28-40.
- 725 [20] Zhao Y-G, Zhang X-Y, Lu Z-H. Complete monotonic expression of the fourth-moment normal
726 transformation for structural reliability. *Computers & Structures*. 2018;196:186-99.
- 727 [21] Zhao Y-G, Ono T. Moment methods for structural reliability. *Structural safety*. 2001;23:47-75.
- 728 [22] Kuang YC, Rajan A, Ooi MP-L, Ong TC. Standard uncertainty evaluation of multivariate polynomial.
729 *Measurement*. 2014;58:483-94.
- 730 [23] Rajan A, Ooi MP-L, Kuang YC, Demidenko SN. Analytical Standard Uncertainty Evaluation Using Mellin
731 Transform. *IEEE Access*. 2015;3:209-22.
- 732 [24] Rajan A, Ooi MP-L, Kuang YC, Demidenko SN, Carstens H. Moment-constrained Maximum Entropy
733 Method for Expanded Uncertainty Evaluation. *IEEE Access*. 2018;6.
- 734 [25] Nikolaidis E, Burdisso R. Reliability based optimization: a safety index approach. *Computers & structures*.
735 1988;28:781-8.
- 736 [26] Enevoldsen I, Sørensen JD. Reliability-based optimization in structural engineering. *Structural safety*.
737 1994;15:169-96.
- 738 [27] Kuschel N, Rackwitz R. Two basic problems in reliability-based structural optimization. *Mathematical*
739 *Methods of Operations Research*. 1997;46:309-33.
- 740 [28] Du X, Chen W. Sequential optimization and reliability assessment method for efficient probabilistic design.
741 *Journal of mechanical design*. 2004;126:225-33.
- 742 [29] Tu J, Choi KK, Park YH. A new study on reliability-based design optimization. *Journal of mechanical*
743 *design*. 1999;121:557-64.
- 744 [30] Youn BD, Choi KK, Park YH. Hybrid analysis method for reliability-based design optimization. *Journal*
745 *of Mechanical Design*. 2003;125:221-32.
- 746 [31] Li F, Wu T, Badiru A, Hu M, Soni S. A single-loop deterministic method for reliability-based design
747 optimization. *Engineering Optimization*. 2013;45:435-58.
- 748 [32] Rashki M, Miri M, Moghaddam MA. A new efficient simulation method to approximate the probability of
749 failure and most probable point. *Structural Safety*. 2012;39:22-9.
- 750 [33] Roudak MA, Shayanfar MA, Barkhordari MA, Karamloo M. A robust approximation method for nonlinear
751 cases of structural reliability analysis. *International Journal of Mechanical Sciences*. 2017;133:11-20.
- 752 [34] Der Kiureghian A, Dakessian T. Multiple design points in first and second-order reliability. *Structural*
753 *Safety*. 1998;20:37-49.
- 754 [35] Lee SH, Kwak BM. Response surface augmented moment method for efficient reliability analysis.
755 *Structural safety*. 2006;28:261-72.
- 756 [36] Lee I, Choi K, Gorsich D. System reliability-based design optimization using the MPP-based dimension
757 reduction method. *Structural and Multidisciplinary Optimization*. 2010;41:823-39.
- 758 [37] Echard B, Gayton N, Lemaire M. AK-MCS: an active learning reliability method combining Kriging and
759 Monte Carlo simulation. *Structural Safety*. 2011;33:145-54.
- 760 [38] Hu C, Youn BD. Adaptive-sparse polynomial chaos expansion for reliability analysis and design of
761 complex engineering systems. *Structural and Multidisciplinary Optimization*. 2011;43:419-42.
- 762 [39] Jin R, Du X, Chen W. The use of metamodeling techniques for optimization under uncertainty. *Structural*
763 *and Multidisciplinary Optimization*. 2003;25:99-116.
- 764 [40] Simpson TW, Poplinski J, Koch PN, Allen JK. Metamodels for computer-based engineering design: survey
765 and recommendations. *Engineering with computers*. 2001;17:129-50.
- 766 [41] Youn BD, Choi KK. A new response surface methodology for reliability-based design optimization.
767 *Computers & structures*. 2004;82:241-56.

- 768 [42] Engelund S, Rackwitz R. A benchmark study on importance sampling techniques in structural reliability.
769 Structural safety. 1993;12:255-76.
- 770 [43] Melchers R. Importance sampling in structural systems. Structural safety. 1989;6:3-10.
- 771 [44] Seo HS, Kwak BM. Efficient statistical tolerance analysis for general distributions using three-point
772 information. International journal of production research. 2002;40:931-44.
- 773 [45] Zhang X, Pandey MD, Zhang Y. Computationally efficient reliability analysis of mechanisms based on a
774 multiplicative dimensional reduction method. Journal of Mechanical Design. 2014;136:061006.
- 775 [46] Xu J, Lu Z-H. Evaluation of moments of performance functions based on efficient cubature formulation.
776 Journal of Engineering Mechanics. 2017;143:06017007.
- 777 [47] Rajan A, Kuang YC, Ooi MP-L, Demidenko SN. Benchmark test distributions for expanded uncertainty
778 evaluation algorithms. IEEE Transactions on Instrumentation and Measurement. 2016;65:1022-34.
- 779 [48] Xu L, Cheng G. Discussion on: moment methods for structural reliability. Structural Safety. 2003;25:193-
780 9.
- 781 [49] Lindsay BG, Basak P. Moments determine the tail of a distribution (but not much else). The American
782 Statistician. 2000;54:248-51.
- 783 [50] Rácz S, Tari Á, Telek M. A moments based distribution bounding method. Mathematical and computer
784 modelling. 2006;43:1367-82.
- 785 [51] Rajan A, Ooi MP-L, Kuang YC, Demidenko SN. Efficient analytical moments for the robustness analysis
786 in design optimisation. The Journal of Engineering: Institution of Engineering and Technology; 2016. p. 423-
787 30.
- 788 [52] Yeun Y, Yang Y, Ruy W, Kim B. Polynomial genetic programming for response surface modeling part 1:
789 a methodology. Structural and Multidisciplinary Optimization. 2005;29:19-34.
- 790 [53] Yeun Y, Kim B, Yang Y, Ruy W. Polynomial genetic programming for response surface modeling part 2:
791 adaptive approximate models with probabilistic optimization problems. Structural and Multidisciplinary
792 Optimization. 2005;29:35-49.
- 793 [54] Nocedal J, Wright SJ. Sequential quadratic programming: Springer; 2006.
- 794 [55] Lee J-O, Yang Y-S, Ruy W-S. A comparative study on reliability-index and target-performance-based
795 probabilistic structural design optimization. Computers & structures. 2002;80:257-69.
- 796 [56] Release M. The MathWorks. Inc, Natick, Massachusetts, United States. 2013;488.
- 797 [57] Missoum S, Ramu P, Haftka RT. A convex hull approach for the reliability-based design optimization of
798 nonlinear transient dynamic problems. Computer methods in applied mechanics and engineering.
799 2007;196:2895-906.
- 800 [58] Hadidi A, Azar BF, Rafiee A. Efficient response surface method for high-dimensional structural reliability
801 analysis. Structural Safety. 2017;68:15-27.
- 802 [59] Zhao D, Xue D. A comparative study of metamodeling methods considering sample quality merits.
803 Structural and Multidisciplinary Optimization. 2010;42:923-38.
- 804 [60] Bucher C, Most T. A comparison of approximate response functions in structural reliability analysis.
805 Probabilistic Engineering Mechanics. 2008;23:154-63.
- 806 [61] Toropov V, Alvarez LF. -Application of genetic programming and response surface methodology to
807 optimization and inverse problems. Inverse Problems in Engineering Mechanics: Elsevier; 1998. p. 551-60.
- 808 [62] Nikolaev NY, Iba H. Regularization approach to inductive genetic programming. IEEE Transactions on
809 evolutionary computation. 2001;5:359-75.
- 810 [63] Searson DP. GPTIPS 2: an open-source software platform for symbolic data mining. Handbook of genetic
811 programming applications: Springer; 2015. p. 551-73.
- 812 [64] Rosenbrock H. An automatic method for finding the greatest or least value of a function. The Computer
813 Journal. 1960;3:175-84.
- 814 [65] Rahman S. A polynomial dimensional decomposition for stochastic computing. International Journal for
815 Numerical Methods in Engineering. 2008;76:2091-116.

- 816 [66] Basudhar A, Missoum S. Adaptive explicit decision functions for probabilistic design and optimization
817 using support vector machines. *Computers & Structures*. 2008;86:1904-17.
- 818 [67] Gavin HP, Yau SC. High-order limit state functions in the response surface method for structural reliability
819 analysis. *Structural safety*. 2008;30:162-79.
- 820 [68] Yang R, Gu L. Experience with approximate reliability-based optimization methods. *Structural and
821 Multidisciplinary Optimization*. 2004;26:152-9.
- 822 [69] Xiao S, Lu Z, Xu L. Multivariate sensitivity analysis based on the direction of eigen space through principal
823 component analysis. *Reliability Engineering & System Safety*. 2017;165:1-10.
- 824 [70] Lee TH, Jung JJ. A sampling technique enhancing accuracy and efficiency of metamodel-based RBDO:
825 Constraint boundary sampling. *Computers & Structures*. 2008;86:1463-76.
- 826 [71] Thanedar PB, Kodiyalam S. Structural optimization using probabilistic constraints. *Structural
827 Optimization*. 1992;4:236-40.
- 828 [72] Styles AJ, Luo FJ, Bai Y, Murray-Parkes JB. Effects of joint rotational stiffness on structural responses of
829 multi-story modular buildings. *Transforming the Future of Infrastructure through Smarter Information:
830 Proceedings of the International Conference on Smart Infrastructure and Construction, 27–29 June 2016*. p. 457-
831 62.
- 832 [73] Innella F, Luo FJ, Bai Y. Capacity of screw connections between plasterboard panels and cold-formed steel
833 for modular buildings. accepted for publication in *Journal of architectural engineering*.
- 834 [74] Lacey AW, Chen W, Hao H, Bi K. Structural response of modular buildings—An overview. *Journal of
835 Building Engineering*. 2017.
- 836 [75] Standard ANZ. *Structural Design Actions. Part 2: Wind Actions: AS-NZS; 2002*.
- 837 [76] Standard ANZ. *Structural Design Actions. Part 0: General Principals: AS-NZS; 2002*.
- 838 [77] Standard ANZ. *Steel Structures. AS-NZS; 2002*.
- 839 [78] ISO C. 13822 Bases for design of structures-Assessment of existing structures. CEN Brussels2005.
- 840 [79] (ABCB) ABCB. *Structural Reliability Handbook*. Canberra ACT2005.
- 841 [80] Safety JCoS. *Probabilistic Model Code*. 2001.
- 842